Behavioral/Systems/Cognitive

Stability of Thalamocortical Synaptic Transmission across Awake Brain States

Carl R. Stoelzel, Yulia Bereshpolova, and Harvey A. Swadlow
Department of Psychology, The University of Connecticut, Storrs, Connecticut 06269

Sensory cortical neurons are highly sensitive to brain state, with many neurons showing changes in spatial and/or temporal response properties and some neurons becoming virtually unresponsive when subjects are not alert. Although some of these changes are undoubtedly attributable to state-related filtering at the thalamic level, another likely source of such effects is the thalamocortical (TC) synapse, where activation of nicotinic receptors on TC terminals have been shown to enhance synaptic transmission *in vitro*. However, monosynaptic TC synaptic transmission has not been directly examined during different states of alertness. Here, in awake rabbits that shifted between alert and non-alert EEG states, we examined the monosynaptic TC responses and short-term synaptic dynamics generated by spontaneous impulses of single visual and somatosensory TC neurons. We did this using spike-triggered current source-density analysis, an approach that enables assessment of monosynaptic extracellular currents generated in different cortical layers by impulses of single TC afferents. Spontaneous firing rates of TC neurons were higher, and burst rates were much lower in the alert state. However, we found no state-related changes in the amplitude of monosynaptic TC responses when TC spikes with similar preceding interspike interval were compared. Moreover, the relationship between the preceding interspike interval of the TC spike and postsynaptic response amplitude was not influenced by state. These data indicate that TC synaptic transmission and dynamics are highly conserved across different states of alertness and that observed state-related changes in receptive field properties that occur at the cortical level result from other mechanisms.

Introduction

Sensory response properties of many cortical neurons are strongly modified by EEG state (Livingstone and Hubel, 1981; Chapin and Lin, 1984; Wörgötter et al., 1998; Edeline et al., 2001; Eyding et al., 2003). Such modulation is seen in anesthetized subjects, in which the EEG is activated by reticular stimulation (Castro-Alamancos, 2002; Castro-Alamancos and Oldford, 2002) and in awake subjects that momentarily shift between alert and non-alert states (Swadlow and Weyand, 1987; Bezdudnaya et al., 2004; Cano et al., 2004). Some of the cortical changes are clearly attributable to changes occurring at the thalamus (Maffei et al., 1965; Coenen and Vendrik, 1972; Bartlett et al., 1973; Singer, 1977; Livingstone and Hubel, 1981), in which EEG state changes are associated with shifts between tonic and burst mode (Weyand et al., 2001; Sherman and Guillery, 2002). These shifts in thalamic mode occur even in awake subjects that shift their level of arousal (Bezdudnaya et al., 2006; Cano et al., 2006). However, there is good reason to believe that additional modulatory influences occur at the level of the cortex, in which changes in cholinergic, adrenergic, and other neuromodulator levels are associated with state shifts (Jiménez-Capdeville and Dykes, 1996; Aston-Jones, 2005).

Notably, the sensitivity to state appears to be considerably greater in some cortical neurons than in thalamocortical (TC) neurons. Thus, although the gain of contrast–response functions and the temporal tuning characteristics of rabbit dorsal lateral geniculate nucleus (LGNd) neurons are very different in alert and non-alert EEG states (Bezdudnaya et al., 2006; Cano et al., 2006), these differences are even stronger in the primary visual cortex (V1), in which some neurons become totally unresponsive in the non-alert state (Bezdudnaya et al., 2004; Cano et al., 2004). One current hypothesis that could account for this is an enhanced TC transmission in the alert state (Gil et al., 1997; Kimura et al., 1999). Nicotinic receptors are present on TC terminals of a wide variety of mammalian orders, including carnivores (Prusky et al., 1987; Parkinson et al., 1988), rodents (Sahin et al., 1992; Bina et al., 1995; Lavine et al., 1997), and primates (Disney et al., 2007). Moreover, nicotine has been shown to enhance the amplitude of postsynaptic TC responses *in vitro* (Gil et al., 1997) and to enhance visual cortical responses in TC recipient layers *in vivo* (Disney et al., 2007). There is, however, no direct evidence that EEG arousal influences synaptic transmission at TC synapses.

To examine this question, we studied the monosynaptic responses that are generated by the cortical synapses formed by single TC neurons, in awake rabbits that shift between non-alert and alert EEG states. We also examined the short-term dynamics of these synapses, which would be expected to vary with variations in presynaptic release (Zucker and Regehr, 2002). We do this in both visual and somatosensory TC systems using spike-triggered current source-density (STCSD) analysis. This method allows measurement of extracellular monosynaptic currents gen-

Received Dec. 16, 2008; revised Jan. 23, 2009; accepted April 23, 2009.
This work was supported by National Institutes of Health Grant EY018251.
Correspondence should be addressed to Harvey A. Swadlow, Department of Psychology, University of Connecticut, 406 Babbidge Road, Box U-1020, Storrs, CT 06269.
DOI:10.1523/JNEUROSCI.5983-08.2009
 0270-6474/09/296851-09$15.00/0

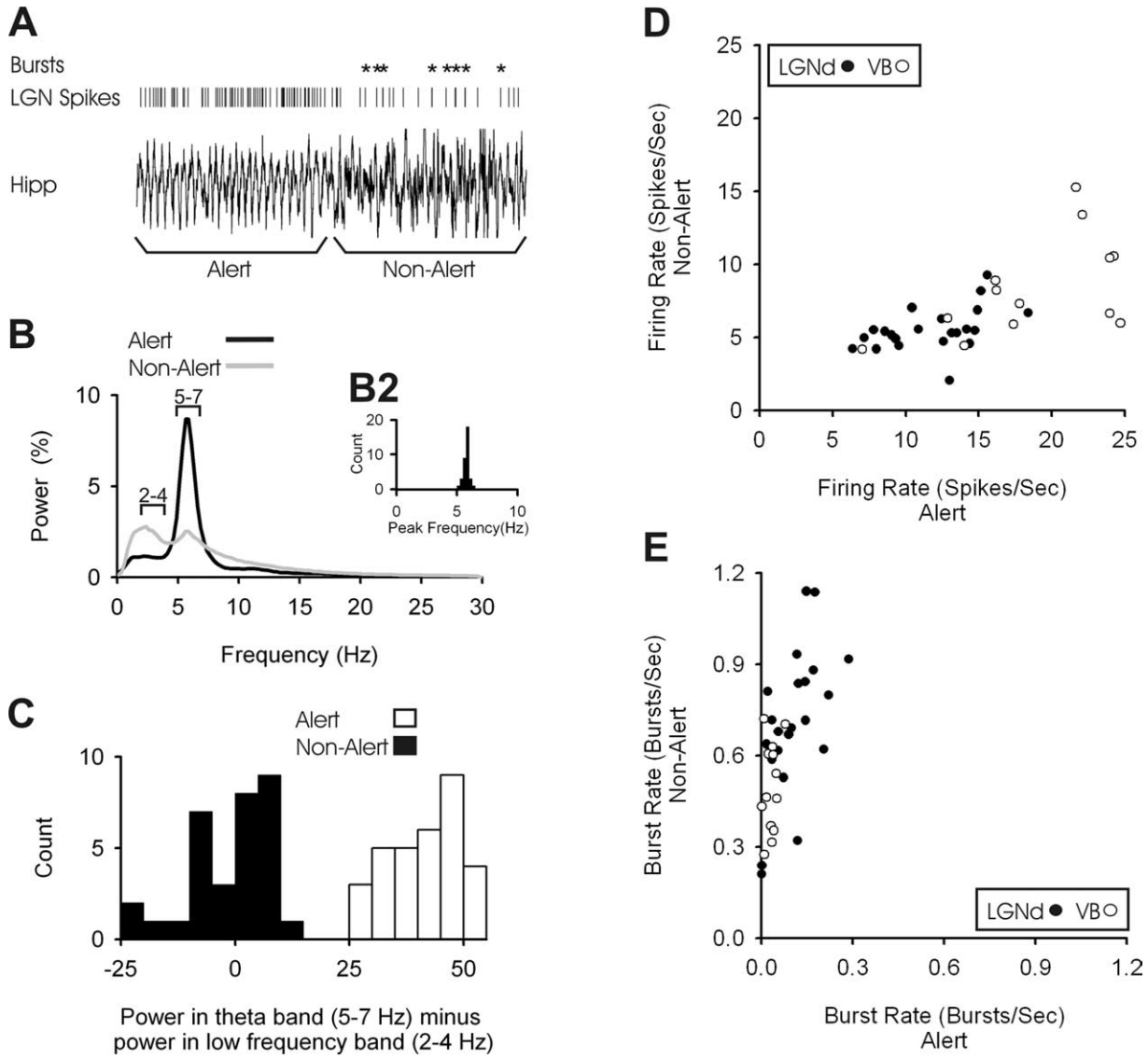

Figure 1. Spontaneous firing rates and burst rates of single thalamic neurons change dramatically during alert and non-alert states. ***A***, A transition from alert to non-alert states as defined by hippocampal EEG. Five seconds of theta activity are shown preceding the transition, followed by 5 s of HVIR. Vertical lines indicate action potentials from a simultaneously recorded LGN cell, with bursts indicated by asterisks. ***B***, For all of our cells, the average of the power spectral density functions of hippocampal EEG during alert (black line) and non-alert (gray line) periods. The *y*-axis shows the percentage of power contained within each bin of 0.25 Hz. The distribution of peak frequencies during alert periods can be seen in ***B2***. ***C***, For both alert and non-alert states, we subtracted the total power in the 2– 4 Hz range from the total power in the 5–7 Hz range. ***D***, The spontaneous firing rates of LGNd (filled circles) and VB (open circles) neurons calculated during alert (*x*-axis) and non-alert (*y*-axis) periods. ***E***, Burst frequency for both LGNd (filled circles) and VB (open circles) neurons during alert (*x*-axis) and non-alert (*y*-axis).

erated in different layers of a topographically aligned cortical column by the impulses of a single TC neuron (Swadlow et al., 2002; Jin et al., 2008; Stoelzel et al., 2008), and the synaptic dynamics of the synapses of these neurons (Swadlow et al., 2002; Stoelzel et al., 2008). Remarkably, although we found that monosynaptic response amplitude was strongly modulated by preceding impulse history, we found no influence of EEG state on the monosynaptic response amplitude or on synaptic dynamics. We found this despite the fact that the thalamus was clearly switching between burst and tonic modes of firing (Sherman and Guillery, 2002) at this state transition.

Materials and Methods

Extracellular recordings were obtained from chronically prepared, adult, Dutch-belted rabbits. Recording in the LGNd and from the retinotopically aligned region of V1 from were obtained from two rabbits and recordings in ventrobasal thalamus (VB) and somatotopically aligned somatosensory cortex (S1) from three rabbits. Initial surgery was performed under anesthesia using aseptic procedures. Subsequent recordings were obtained in the awake state using procedures approved by the Institutional Animal Care and Use Committee at the University of Connecticut in accordance with National Institutes of Health guidelines. Methods used to ensure the comfort of our subjects have been described in detail previously (Swadlow et al., 2002). Rabbits were held snugly within a stocking and were placed on a rubber pad. The steel bar on the head was fastened to a restraining device in a manner that minimized stress on the neck. Rabbits generally sat quietly for several hours of each recording session and were then returned to their home cage.

Physiological recordings. Spike data and cortical and hippocampal EEG activity were acquired using a Plexon data acquisition system. Thalamic microelectrodes were constructed of quartz-insulated, platinum–tungsten filaments (Reitboeck, 1983) (stock diameter of 40 μm), pulled to a taper and sharpened to a fine tip. A concentric array of seven such inde-

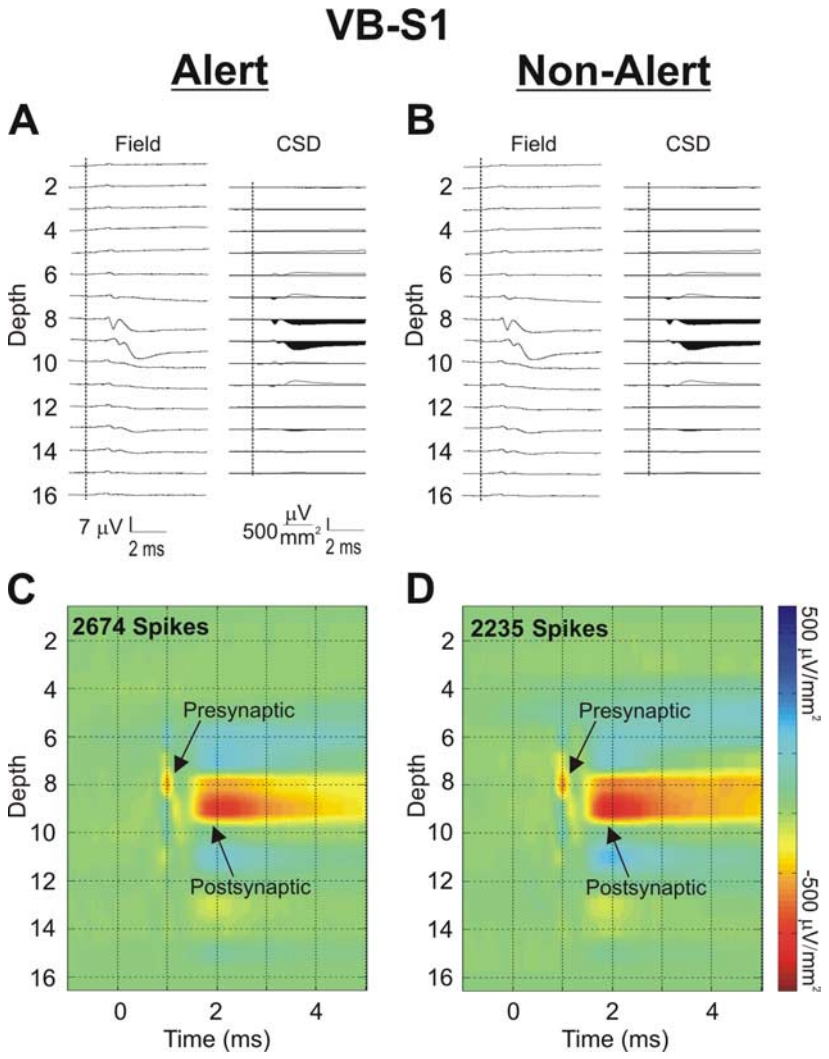

Figure 2. The monosynaptic response generated in cortical layer 4 by single thalamic neurons is the same in alert and non-alert brain states. ***A***, An example, in the alert state, of the spike-triggered LFP (left) and STCSD (right) depth profiles generated in an S1 barrel column by impulses of a VB thalamic neuron located in the topographically aligned VB thalamic barreloid. The vertical dashed lines indicate the time of the TC spike. Only spikes having a preceding interspike interval between 100 and 200 ms were used. ***B***, The same measures as in ***A*** but taken in the non-alert state. For both the alert (***C***) and non-alert (***D***) states, a color map was applied to the STCSD depth profiles. Gain settings and color intensities for these spike-triggered LFPs and STCSD profiles are identical in both states.

pendently movable electrodes (~150 μm spacing) was chronically implanted within either LGNd or VB thalamus. Electrodes were each under microdrive control and were guided within fine-diameter (~150 μm outer diameter) stainless steel tubes (Swadlow et al., 2005). Recording sessions usually lasted 4–8 h, during which the synaptic impact of one or more thalamic neurons was thoroughly studied.

Cortical field potential and multiunit recordings were obtained using 16-channel silicone probes (NeuroNexus Technologies). Probe sites were separated vertically by 100 μm, had surface areas of 700 μm^2, and impedances of 0.3–0.8 MΩ. Spike data from the probe sites usually consisted of low-amplitude multiunit activity, used for plotting receptive fields. Field potentials at each site were filtered at 2 Hz to 1.9 kHz (half-amplitude) and sampled continuously at 5 kHz. For visual cortex, recordings were obtained from monocular regions of V1 that lie within 10° of the visual streak (the visual horizon) (Levick, 1967), and for somatosensory cortex, recordings were made in barrel cortex. Hippocampal EEG was recorded via platinum–iridium microwires. Thalamocortical "bursts" were defined as clusters of at least two spikes with interspike intervals of ≤4 ms, in which the initial spike had a preceding interspike interval of at least 100 ms (Lu et al., 1992).

The success of these experiments depended on achieving precise topographic alignment between the thalamic and cortical recording site. After obtaining stable recordings from one or more thalamic neurons, sensory cortex was mapped using a finely tapered microelectrode (60 μm maximal diameter) until retinotopic/topographic alignment was achieved (Swadlow et al., 2002; Stoelzel et al., 2008). This electrode was then replaced with the 16-channel probe. The dura was always left intact. In some penetrations, layer 6 probe sites were identified by antidromic activation of corticogeniculate neurons via microstimulation (<10 μA) via the LGNd electrodes (Swadlow et al., 2002).

EEG state. Hippocampal EEG activity provided the index of alert versus non-alert states. Hippocampal activity in the rabbit can generally be separated into theta activity (4–8 Hz) and high-voltage, irregular activity (HVIR). Hippocampal theta activity is associated with cortical desynchronization in an aroused, alert state, whereas HVIR is associated with cortical synchronization in a nona-roused, non-alert state (Green and Arduini, 1954; Swadlow and Gusev, 2001). During our recordings, rabbits often alternated spontaneously between theta and HVIR activity. Low-intensity auditory or tactile stimulation was occasionally used to quickly convert HVIR activity into theta activity. After the recording session, EEG records were manually segmented into alert segments containing theta and non-alert segments containing HVIR activity. Segmentation of hippocampal EEG was then evaluated through fast Fourier transform analysis of the selected segments, and the power in the peak theta range (5–7 Hz) was compared with the power in the range of 2–4 Hz (Swadlow and Gusev, 2001; Bezdudnaya et al., 2006; Cano et al., 2006). We also regularly examined the EEG recorded on cortical channels to ensure ourselves that the cortical and hippocampal EEG was appropriately correlated (above).

Spike-triggered current source-density analyses. Depth profiles of the synaptic impact of TC impulses were generated using methods described previously (Swadlow et al., 2002; Stoelzel et al., 2008). Spike-triggered averages of the cortical field activity were generated from the spontaneous impulse activity of TC neurons. As described in Results, it was important to ensure that comparisons of monosynaptic response amplitude across brain states were made only for responses generated by TC impulses with similar preceding interspike intervals. To allow this, we compared only spikes with short (5–20 ms), medium (100–200 ms), or long (500–3000 ms) preceding interspike intervals. The long interspike intervals were relatively rare, and we required a minimum of 100 spikes within each state for each of these interval ranges. The peak amplitude of the postsynaptic response was measured only during the initial 1 ms after the onset of the postsynaptic response, to avoid the possibility of including disynaptic currents.

For analysis of synaptic dynamics, STCSD depth profiles generated from spikes with short preceding interspike intervals (5–20 ms) were compared with those generated by spikes with long preceding intervals (500–3000 ms). We eliminated spikes with very short (<5 ms) subsequent interspike intervals to avoid generating compound averages from high-frequency spikes.

STCSD profiles were generated from the field profiles according to the method described by Freeman and Nicholson (1975). First, we dupli-

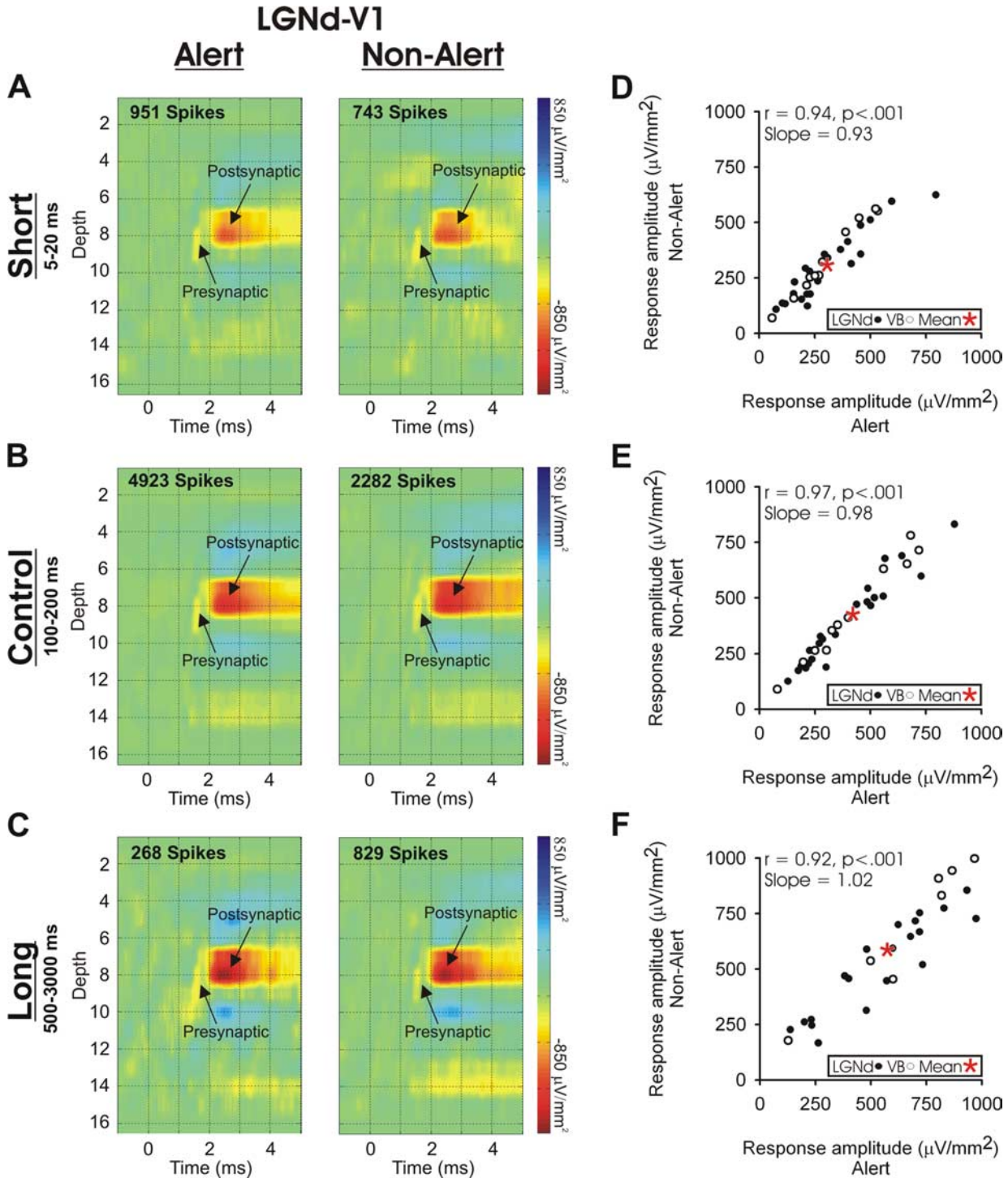

Figure 3. The monosynaptic response generated in cortical layer 4 by single thalamic neurons does not change with brain state but does change with preceding interspike interval. ***A–C***, STCSD depth profiles generated in V1 during alert (left) and non-alert (right) brain states by spikes of a topographically aligned LGNd neuron. The cortical responses are shown that were generated by LGNd spikes with preceding interspike intervals that were short (5–20 ms; ***A***), intermediate (100 –200 ms; ***B***), or long (500 –3000 ms; ***C***). The color gain settings are identical for each panel. ***D–F***, For all of the VB and LGNd neurons studied, the amplitude of the monosynaptic responses generated in the cortex are shown for TC impulses that had preceding interspike intervals that were short (5–20 ms; ***D***), intermediate (100 –200 ms; ***E***), or long (500 –3000 ms; ***F***). Response amplitudes did not differ between alert (*x*-axis) and non-alert (*y*-axis) states. In ***D*** and ***E***, the mean amplitude of the monosynaptic response for each state is indicated by the asterisks.

cated the uppermost and lowermost field trace (Vaknin et al., 1988), which converted our 16 recording channels to a total of 18 channels. Next, we smoothed (Freeman and Nicholson, 1975) to reduce high spatial-frequency noise components. This eliminated two of the 18 traces. For smoothing,

$$\bar{\varphi}(r) = \frac{1}{4}\left(\varphi(r+h) + 2\varphi(r) + \varphi(r-h)\right),$$

where φ is the field potentials, r is the coordinate perpendicular to the layers, h is the sampling interval (100 μm).

Next, we calculated the second derivative, and this yielded a total of 14 traces. For the second derivative,

$$D = \frac{1}{h^2}\left(\bar{\varphi}(r + h) - 2\bar{\varphi}(r) + \bar{\varphi}(r - h)\right).$$

In the STCSD profiles, current sinks are indicated by downward deflections and sources by upward deflections. To facilitate visualization of STCSD profiles, we generated color image plots. These were plotted by linear interpolation along the depth axis, red and blue representing current sinks and sources, respectively. Green is ~0, normalized to the 1 ms period before the thalamic spike.

Cross-correlation analysis of TC–interneuron pairs. All data were collected in the absence of peripheral stimulation, under conditions of spontaneous activity. Putative fast-spike inhibitory interneurons were identified by their high-frequency discharge (>600 Hz) of three or more spikes after electrical stimulation of the thalamus and their brief spike duration (Swadlow and Gusev, 2002). Cross-correlograms were generated from spontaneous thalamic spikes with preceding interspike intervals between 100 and 200 ms. We selected a brief window (±0.6 ms on each side of the peak of the cross-correlogram) for calculation of efficacy values. We restricted our analysis to this brief window because peaks in the thalamocortical cross-correlogram in both the somatosensory (Swadlow, 1995) and visual (Reid and Alonso, 1995; Alonso et al., 2001) systems are comparably short and because we wanted to limit the analysis to the effects of a single presynaptic impulse. Efficacy values were calculated by counting the number of action potentials that occurred in the cortical neuron during this brief temporal window, subtracting a baseline number of spikes expected by chance during this period and dividing this value by the number of triggering thalamic spikes. The number of cortical spikes expected by chance was based on the mean number of spikes per bin that occurred between −4 and +1 ms of the thalamic spike time. We limited our analysis to those thalamocortical pairs with efficacy values >2%. This efficacy value is considerably higher than the median efficacy value for TC–fast-spike interneuron synaptic contacts in the rabbit S1 (1.2%) (Swadlow and Gusev, 2002). Here, we needed to select pairs with relatively high efficacy values because we were filtering our spike trains considerably. Thus, our measurements generally yielded approximately one-third of the spikes in the alert state, one-third in the non-alert state, and one-third in an ambiguous state, which we rejected from analysis. Moreover, from the one-third of the spikes that were included in each state, we analyzed only those spikes with comparable preceding interspike intervals of 100–200 ms). This further reduced the spike counts greatly. For these reasons, we need to begin with reasonably strong connections so results, after the stringent selection of spikes to be used, would not be lost in the noise.

Results

Rabbits were awake during our recordings and regularly transitioned between alert and non-alert state. A representative hippocampal EEG trace is presented in Figure 1*A*, where the rabbit shifted rapidly from the alert to the non-alert state. The spike train of one LGNd neuron is seen above the EEG trace, with bursts indicated by the asterisks. To validate our EEG-based measures of state, we examined the state-related behavior of the 22 LGNd neurons and 13 VB neurons that were used to examine the effects of state on TC responses. The mean power spectral density function for alert and non-alert EEG segments is shown in Figure 1*B*. The power spectral density for alert segments always peaked between 5 and 7 Hz (Fig. 1*B2*). For both alert and non-alert segments, we measured the relative power contained within the 2–4 Hz range and subtracted that from the relative power contained in the 5–7 Hz range (theta); the distribution of these power differences is shown in Figure 1*C*. As was found in previous studies of TC neurons (Swadlow and Gusev, 2001; Bezdudnaya et al., 2006), shifts from the alert to non-alert state were accompanied by a prominent decrease in spontaneous firing rate (Fig. 1*D*) ($p < 0.001$), coupled with a large (eightfold) increase in the amount of burst activity (Fig. 1*E*) ($p < 0.001$). These strong shifts in spontaneous activity and bursting make it clear that our EEG measures reflect a clear shift in state.

We studied the monosynaptic impact generated in layer 4 by the impulses of 22 LGNd neurons and 11 VB neurons. For each TC neuron, we found the retinotopic (LGNd neurons) or vibrissotopic (VB neurons) region of cortex and, using a multisite vertical probe (16-channels; see Material and Methods), recorded the depth profile of the cortical EEG during spontaneous activity of the thalamic neurons. From this, we calculated the spike-triggered local field potentials (LFPs) and then the STCSD (Material and Methods). This yielded a measure of the presynaptic (axonal) and postsynaptic currents generated through the cortical layers by these single thalamic neurons (Swadlow et al., 2002; Stoelzel et al., 2008). For a number of reasons, we are confident that our measures of the axonal and postsynaptic responses from STCSD reflect the responses generated by single TC axons (supplemental Material and Methods, available at www.jneurosci.org as supplemental material). Here, we examine only those currents generated within layer 4, within the initial 1 ms of the postsynaptic response.

We have shown previously that the amplitude of monosynaptic cortical responses generated by VB and LGNd impulses is strongly related to the preceding interspike interval, with long intervals yielding stronger responses (Swadlow et al., 2002; Stoelzel et al., 2008). This occurs because TC synapses, *in vivo*, are in a chronic state of depression (attributable to high spontaneous firing rates) that is relieved by long preceding interspike intervals (Ramcharan et al., 2000; Swadlow and Gusev, 2001; Castro-Alamancos, 2002; Castro-Alamancos and Oldford, 2002; Swadlow et al., 2002; Boudreau and Ferster, 2005; Stoelzel et al., 2008). In the present analyses, therefore, it was essential to control for the different interspike interval distributions that accompany state changes. Otherwise, a change in postsynaptic response amplitude could be attributed to state, when in fact it was simply attributable to state-related changes in the mean preceding interspike interval. To do this, in both states, we selected only those action potentials that had similar preceding interspike intervals.

Figure 2, *A* and *B*, presents, in the alert and non-alert states, respectively, the laminar profile of spike-triggered LFPs (left) and STCSDs (right) generated in an S1 barrel by a VB thalamic neuron in the topographically aligned VB barreloid. Figure 2, *C* and *D*, shows the colorized STCSD depth profiles in the alert and non-alert states, respectively. Here, we present the results only for those spikes with preceding interspike intervals of 100–200 ms, which are most numerous in both states. Notably, there is almost no difference between the responses generated in the alert and non-alert states.

Figure 3*A–C* shows an example from an LGNd neuron generating a presynaptic and postsynaptic impact in the retinotopically aligned region of V1. Here we present only the colorized depth profile of the STCSDs seen in each state, but we do so for LGNd impulses with preceding interspike intervals that are short [5–20 ms (*A*)], medium [100–200 ms (*B*)], and long [500–3000 ms (*C*)]. There is a clear within-state effect of preceding interspike interval, with the longest intervals having the strongest postsynaptic effect. This was expected because of the recovery from synaptic depression at the longer intervals (Swadlow and Gusev, 2001; Swadlow et al., 2002; Boudreau and Ferster, 2005; Stoelzel et al., 2008). However, no effect of state can be seen.

Figure 3*D–F* compares, for each of our LGNd and VB neurons, the monosynaptic TC response amplitude generated in

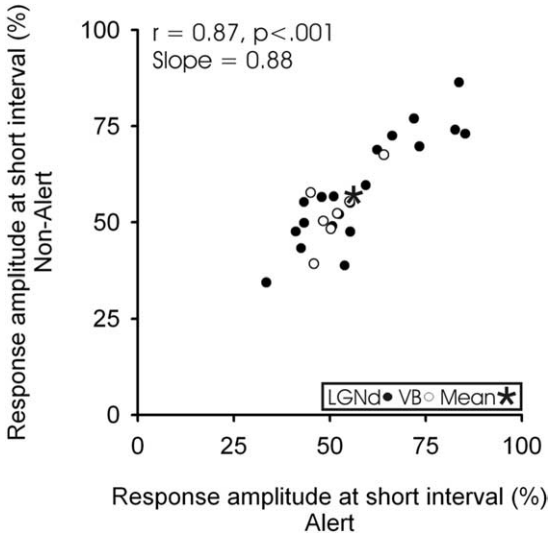

Figure 4. Synaptic dynamics at the TC synapse do not change with brain state. Data are shown for both visual (filled circles) and somatosensory (open circles) systems and in the alert (*x*-axis) and non-alert (*y*-axis) states. Points represent the degree of reduction (percentage) in postsynaptic responses that were generated by thalamic spikes with short preceding intervals (5–20 ms) versus spikes with long preceding intervals (500–3000 ms). The asterisks indicates the mean degree of synaptic depression within each state.

layer 4 in the alert and non-alert states from spikes with a preceding interspike interval of 5–20 ms (*D*), 100–200 ms (*E*) or 500–3000 ms (*F*). The postsynaptic responses to thalamic impulses with similar preceding interspike intervals were very similar in the two states. For spikes with a preceding interspike interval between 100 and 200 ms (Fig. 3*E*), the amplitude was 1.2% greater during the non-alert state, but this was not significant (paired *t* test, $t = 0.769$; $p < 0.448$). The slope of this correlation (slope of 0.98; $r = 0.97$; $n = 33$; $p < 0.001$) between the amplitude of the responses in these states shows that cortical state has little effect on monosynaptic TC transmission. Similarly, no effect of state could be seen in the slopes of the correlations for the short interspike interval condition (slope of 0.93) or the longer interspike interval condition (slope of 1.02). Note that spikes with long preceding interspike intervals are fairly rare (Stoelzel et al., 2008, their Fig. 5), and six of our TC neurons (four VB and two LGNd) did not have at least 100 spikes at this interval in each state tested and were excluded from the long interval analysis (see Materials and Methods).

As noted above, TC synapses exhibit activity-dependent depression (Gil et al., 1997; Swadlow and Gusev, 2001; Castro-Alamancos and Oldford, 2002; Swadlow et al., 2002; Boudreau and Ferster, 2005; Stoelzel et al., 2008), and this can seen by comparing the mean monosynaptic response amplitude for each interval condition (Fig. 3*E*,*F*, red asterisks). We asked whether the level of this depression differed in the alert versus non-alert states. We measured depression at the TC synapse by comparing the response amplitude generated from these short interval spikes as a percentage reduction from the response amplitude from spikes with long preceding interspike intervals (Fig. 4). The six TC neurons excluded from the long interval analysis were similarly excluded from this analysis. All remaining TC neurons showed some reduction in response amplitude from short interval spikes. However, although the amplitude of the responses of all of our cells were reduced at short preceding interspike intervals in both alert (43.8%; paired *t* test, $t = 9.329$; $p < 0.001$) and non-alert (43.1%; paired *t* test, $t = 10.178$; $p < 0.001$) states, the degree of the reduction (the depression) did not significantly differ between these two states (paired *t* test, $t = -0.570$; $p = 0.574$).

The above analyses using the STCSD method examines monosynaptic currents generated by single TC axons. Because ~90% of TC synaptic contacts are onto excitatory neurons (Freund et al., 1989; Staiger et al., 1996; Erisir and Dreusicke, 2005), it is reasonable to conclude that our STCSD measures are dominated by synaptic contacts onto excitatory populations and that any contribution of TC synapses onto inhibitory cells may be obscured in the averaged population response. Because inhibitory neurons may respond differently to the neuromodulators associated with the alert versus non-alert states (Bacci et al., 2005), we thought it would be useful to examine any state-related differences in the TC impact onto inhibitory interneurons. Because the STCSD method is insensitive to postsynaptic cell class, we used cross-correlation analysis to achieve this. Fast-spike interneurons of layer 4 receive a significant input from topographically aligned TC neurons (Swadlow, 1995; Bruno and Simons, 2002; Swadlow and Gusev, 2002). We examined the state-related TC synaptic efficacy for seven such neurons (four somatosensory, three visual), each of which had synaptic efficacy of >2% (see Material and Methods). Examples from correlograms from each state (at comparable interspike intervals of 100–200 ms) can be seen in Figure 5*A*. As was the case for the STCSD analysis, we found no effect of state on the TC synaptic efficacy onto putative inhibitory interneurons of S1 or V1 (Fig. 5*B*). The examination of only stronger connections (efficacy values of >2%) raises the possibility that our results might be affected by a ceiling effect, whereby additional gains in synaptic transmission were not possible. However, the synaptic efficacy in all seven connected pairs was strongly affected of preceding interspike interval. Efficacy was lowest from TC spikes with short preceding interspike intervals and highest from TC spikes with long preceding interspike intervals (percentage reduction: S1, 68.3%; V1, 46.2%), thus demonstrating that significant gains in synaptic strength above control level were detectable when the preceding interspike was long.

Discussion

As we have shown previously, the spontaneous firing rate of TC neurons was reduced and burst rate was greatly increased in the non-alert state (Swadlow and Gusev, 2001; Bezdudnaya et al., 2006). These observations indicate that our EEG-defined measures of state are of great consequence to the thalamus and suggest that thalamic neurons are primarily in tonic mode in the alert state and in burst mode in the non-alert state (Sherman and Guillery, 2002). Our results also confirm previous *in vivo* findings showing enhanced monosynaptic responses generated by single TC neurons after long preceding interspike intervals, indicating relief from a chronic depression of the TC synapse (Swadlow and Gusev, 2001; Swadlow et al., 2002; Boudreau and Ferster, 2005; Stoelzel et al., 2008). However, our results provide no support for the notion that TC synaptic transmission is enhanced when non-alert subjects shift to an alert state, in either the visual or the somatosensory TC system. Thus, when comparing TC spikes with similar preceding intervals, we found no state-related change in the amplitude of monosynaptic currents that were generated (Figs. 2, 3), and this conclusion was supported by our more limited analysis of TC efficacy onto putative cortical fast-spike interneurons (Fig. 5). Given the consistency of TC synaptic transmission across states, it is not surprising that we saw no state-related difference in synaptic dynamics (Fig. 4).

The state invariance of TC postsynaptic response amplitude

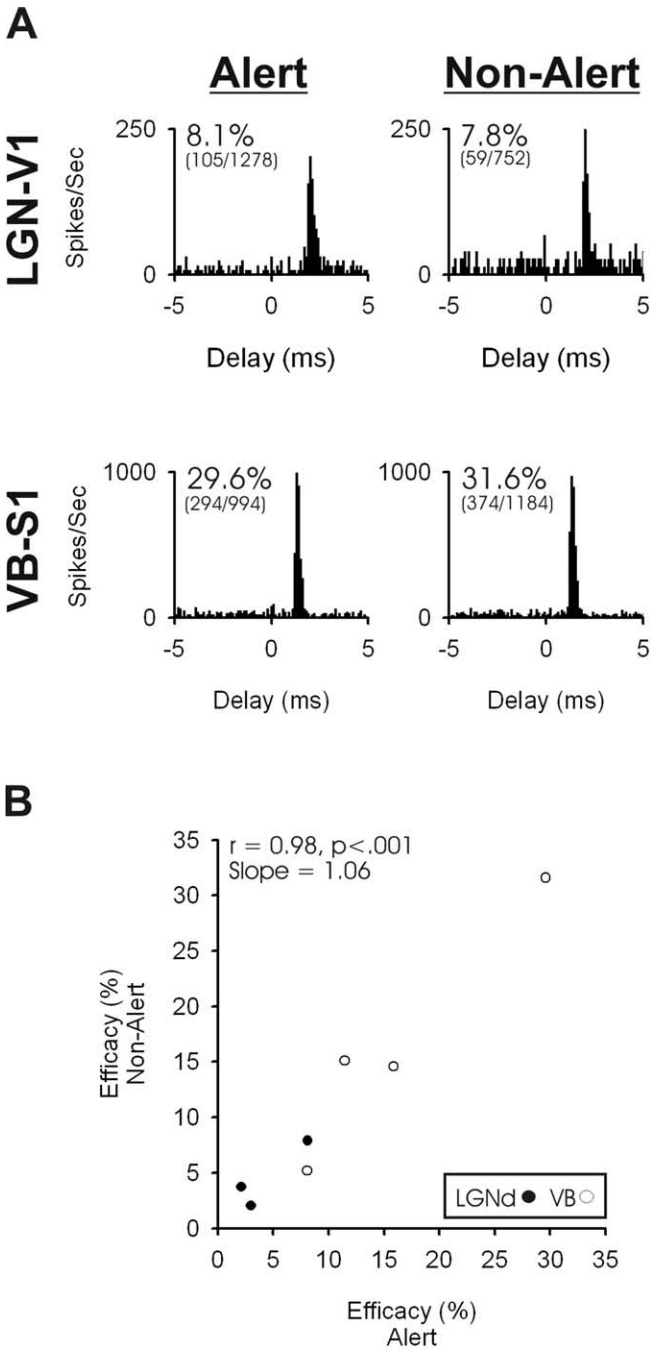

Figure 5. TC activation of fast-spike inhibitory interneurons is also independent of behavioral state. ***A***, Examples of cross-correlograms generated in the alert state (left) and non-alert state (right) for an LGN–V1 pair (top) and a VB–S1 pair (bottom). ***B***, The TC synaptic efficacy of four somatosensory and three visual TC– cortical pairs during alert (*x*-axis) and non-alert (*y*-axis) periods. These state comparisons of synaptic efficacy are based on TC spikes with preceding interspike intervals of 100–200 ms.

was surprising for several reasons. EEG state changes are associated with considerable variations in the release of cortical neuromodulators (Jiménez-Capdeville and Dykes, 1996; Aston-Jones 2005), some of which would be expected, through presynaptic and/or postsynaptic mechanisms, to influence TC responses. One potential presynaptic mechanism has gained some currency in this regard: the modulation of TC transmission via activation of the nicotinic receptors that are found on TC terminals in a variety of mammalian orders (Prusky et al., 1987; Parkinson et al., 1988; Sahin et al., 1992; Bina et al., 1995; Lavine et al., 1997; Disney et al., 2007). Thus, *in vitro*, Gil et al. (1997) reported enhancement of TC EPSPs in S1 layer 4 neurons after application of nicotinic agonists. *In vivo*, application of nicotine into layer 4c of the anesthetized monkey results in an increased neuronal responsiveness to low-contrast visual stimuli (Disney et al., 2007), and a similar enhancement has been reported in layer 4 of auditory cortex (Liang et al., 2008) after systemic administration of nicotine. Because of these results, we were very surprised to see no modulation of postsynaptic response amplitude when rabbits shifted between alert and non-alert states. Importantly, as noted above, this state-change is sufficient to shift thalamic neurons between burst and tonic mode and to strongly modulate the visual response properties of thalamic neurons (Bezdudnaya et al., 2006; Cano et al., 2006).

Given the above results *in vitro* (Gil et al., 1997) and in anesthetized animals (Disney et al., 2007; Liang et al., 2008), one possible reason for the stability of postsynaptic responses across different awake states is that basal acetylcholine levels in awake subjects (both alert and non-alert) may be much higher than in anesthetized subjects (this possibility was noted by Disney et al., 2007). If so, cholinergic levels in awake but non-alert subjects may have reached an asymptote vis-à-vis the nicotinic receptors on TC terminals (which may not be the case for intracortical muscarinic receptors), and any incremental increase in cholinergic release that occurs when shifting from the non-alert to the alert state may have little effect on TC synaptic transmission.

Thalamocortical and intracortical synapses show differences in their sensitivity to various neuromodulators, which are released in a state-dependent manner. This has led to suggestions that the balance of thalamic versus cortical synaptic drive onto cortical neurons may be state dependent, with greater control by the thalamus in alert states, when neuromodulator levels are high (Hasselmo, 1995; Gil et al., 1997; Kimura, 2000). Our findings of state-independent TC transmission do not preclude such a state-related shift in TC versus cortical drive to cortical neurons. Our results do indicate, however, that state-related changes in TC synaptic transmission are unlikely to provide the underlying mechanism for such a shift. Recently, a shift in the relative potency of thalamic and intracortical drive onto cortical neurons was proposed to occur under different conditions of visual stimulation (Nauhaus et al., 2009). This shift, however, is thought to result from stimulus-related changes in the efficacy of horizontal cortical connectivity.

Many cortical neurons show dramatic changes in sensory responses with shifts between alert and non-alert EEG states (Swadlow and Weyand, 1987; Wörgötter et al., 1998; Castro-

Alamancos, 2002; Bezdudnaya et al., 2004; Cano et al., 2004; Castro-Alamancos, 2004). Our results suggest that such state-dependant changes in the sensory-evoked responsiveness of cortical neurons cannot be explained by state-related modulation of TC synaptic transmission. Instead, TC synaptic transmission is here viewed as being highly conserved across state shifts that occur in awake subjects. At the same time, however, TC transmission is strongly modulated by variations in interspike interval, through mechanisms of short-term synaptic depression (Gil et al., 1997; Swadlow and Gusev, 2001; Castro-Alamancos and Oldford, 2002; Swadlow et al., 2002; Boudreau and Ferster, 2005; Stoelzel et al., 2008). Because, as we have shown, the interval distribution of TC spikes changes dramatically when alert subjects shift to the non-alert state, we could conclude that state indirectly effects the distribution of postsynaptic response amplitudes generated by single TC neurons. However, our results indicate that shifts in cortical response properties that are observed during such state shifts are likely attributable to factors other than changes in TC monosynaptic response amplitude. Such factors may include an inheritance/amplification of changes that are known to occur at the level of the thalamus (Bezdudnaya et al., 2006; Cano et al., 2006; Swadlow and Weyand, 1985), changes in the degree of synchrony of convergent thalamic inputs (Kawai et al., 2007), and/or the effect of arousal-related neuromodulators on postsynaptic neurons.

References

Alonso JM, Usrey WM, Reid RC (2001) Rules of connectivity between geniculate cells and simple cells in cat primary visual cortex. J Neurosci 21:4002–4015.

Aston-Jones G (2005) Brain structures and receptors involved in alertness. Sleep Med 6 [Suppl 1]:S3–S7.

Bacci A, Huguenard JR, Prince DA (2005) Modulation of neocortical interneurons: extrinsic influences and exercises in self-control. Trends Neurosci 28:602–610.

Bartlett JR, Doty RW, Pecci-Saavedra J, Wilson PD (1973) Mesencephalic control of lateral geniculate nucleus in primates 3. Modifications with state of alertness. Exp Brain Res 18:214–224.

Bezdudnaya T, Cano M, Swadlow HA, Alonso JM (2004) Temporal frequency tuning of excitatory and inhibitory neurons in alert and drowsy visual cortex. Soc Neurosc Abstr 30:410.5.

Bezdudnaya T, Cano M, Bereshpolova Y, Stoelzel CR, Alonso JM, Swadlow HA (2006) Thalamic burst mode and inattention in the awake LGNd. Neuron 49:421–432.

Bina KG, Guzman P, Broide RS, Leslie FM, Smith MA, O'Dowd DK (1995) Localization of {alpha} 7 nicotinic receptor subunit mRNA and {alpha}-bungarotoxin binding sites in developing mouse somatosensory thalamocortical system. J Comp Neurol 363:321–332.

Boudreau CE, Ferster D (2005) Short-term depression in thalamocortical synapses of cat primary visual cortex. J Neurosci 25:7179–7190.

Bruno RM, Simons DJ (2002) Feedforward mechanisms of excitatory and inhibitory cortical receptive fields. J Neurosci 22:10966–10975.

Cano M, Bezdudnaya T, Swadlow HA, Alonso JM (2004) Contrast sensitivity of excitatory and inhibitory neurons in alert and drowsy visual cortex. Soc Neurosci Abstr 30:410.4.

Cano M, Bezdudnaya T, Swadlow HA, Alonso JM (2006) Brain state and contrast sensitivity in the awake visual thalamus. Nat Neurosci 9:1240–1242.

Castro-Alamancos MA (2002) Role of thalamocortical sensory suppression during arousal: focusing sensory inputs in neocortex. J Neurosci 22:9651–9655.

Castro-Alamancos MA (2004) Absence of rapid sensory adaptation in neocortex during information processing states. Neuron 41:455–464.

Castro-Alamancos MA, Oldford E (2002) Cortical sensory suppression during arousal is due to the activity-dependent depression of thalamocortical synapses. J Physiol 541:319–331.

Chapin JK, Lin CS (1984) Mapping the body representation in the SI cortex of anesthetized and awake rats. J Comp Neurol 229:199–213.

Coenen AM, Vendrik AJ (1972) Determination of the transfer ratio of cat's geniculate neurons through quasi-intracellular recordings and the relation with the level of alertness. Exp Brain Res 14:227–242.

Disney AA, Aoki C, Hawken MJ (2007) Gain modulation by nicotine in macaque V1. Neuron 56:701–713.

Edeline JM, Dutrieux G, Manunta Y, Hennevin E (2001) Diversity of receptive field changes in auditory cortex during natural sleep. Eur J Neurosci 14:1865–1880.

Erisir A, Dreusicke M (2005) Quantitative morphology and postsynaptic targets of thalamocortical axons in critical period and adult ferret visual cortex. J Comp Neurol 485:11–31.

Eyding D, Macklis JD, Neubacher U, Funke K, Wörgötter F (2003) Selective elimination of corticogeniculate feedback abolishes the electroencephalogram dependence of primary visual cortical receptive fields and reduces their spatial specificity. J Neurosci 23:7021–7033.

Freeman JA, Nicholson C (1975) Experimental optimization of current source-density technique for anuran cerebellum. J Neurophysiol 38:369–382.

Freund TF, Martin KA, Soltesz I, Somogyi P, Whitteridge D (1989) Arborization pattern and postsynaptic targets of physiologically identified thalamocortical afferents in striate cortex of the macaque monkey. J Comp Neurol 289:315–336.

Gil Z, Connors BW, Amitai Y (1997) Differential regulation of neocortical synapses by neuromodulators and activity. Neuron 19:679–686.

Green JD, Arduini AA (1954) Hippocampal electrical activity in arousal. J Neurophysiol 17:533–557.

Hasselmo ME (1995) Neuromodulation and cortical function: modeling the physiological basis of behavior. Behav Brain Res 67:1–27.

Jiménez-Capdeville ME, Dykes RW (1996) Changes in cortical acetylcholine release in the rat during day and night: differences between motor and sensory areas. Neuroscience 71:567–579.

Jin JZ, Weng C, Yeh CI, Gordon JA, Ruthazer ES, Stryker MP, Swadlow HA, Alonso JM (2008) On and Off domains of geniculate afferents in cat primary visual cortex. Nat Neurosci 11:88–94.

Kawai H, Lazar R, Metherate R (2007) Nicotinic control of axon excitability regulates thalamocortical transmission. Nat Neurosci 10:1168–1175.

Kimura F (2000) Cholinergic modulation of cortical function: a hypothetical role in shifting the dynamics in cortical network. Neurosci Res 38:19–26.

Kimura F, Fukuda M, Tsumoto T (1999) Acetylcholine suppresses the spread of excitation in the visual cortex revealed by optical recording: possible differential effect depending on the source of input. Eur J Neurosci 11:3597–3609.

Lavine N, Reuben M, Clarke PBS (1997) A population of nicotine receptors is associated with thalamocortical afferents in the adult rat: laminar and areal analysis. J Comp Neurol 380:175–190.

Levick WR (1967) Receptive fields and trigger features of ganglion cells in the visual streak of the rabbits retina. J Physiol 188:285–307.

Liang K, Poytress BS, Weinberger NM, Metherate R (2008) Nicotinic modulation of tone-evoked responses in auditory cortex reflects the strength of prior auditory learning. Neurobiol Learn Mem 90:138–146.

Livingstone MS, Hubel DH (1981) Effects of sleep and arousal on the processing of visual information in the cat. Nature 291:554–561.

Lu SM, Guido W, Sherman SM (1992) Effects of membrane voltage on receptive field properties of lateral geniculate neurons in the cat: contributions of the low threshold Ca^{2+} conductance. J Neurophysiol 68:2185–2198.

Maffei L, Moruzzi G, Rizzolatti G (1965) Influence of sleep and wakefulness on the response of lateral geniculate units to sinewave photic stimulation. Arch Ital Biol 103:596–608.

Nauhaus I, Busse L, Carandini M, Ringach DL (2009) Stimulus contrast modulates functional connectivity in visual cortex. Nat Neurosci 12:70–76.

Parkinson D, Kratz KE, Daw NW (1988) Evidence for a nicotinic component to the actions of acetylcholine in cat visual cortex. Exp Brain Res 73:553–568.

Prusky GT, Shaw C, Cynader MS (1987) Nicotine receptors are located on lateral geniculate nucleus terminals in cat visual cortex. Brain Res 412:131–138.

Ramcharan EJ, Cox CL, Zhan XJ, Sherman SM, Gnadt JW (2000) Cellular mechanisms underlying activity patterns in the monkey thalamus during visual behavior. J Neurophysiol 84:1982–1987.

Reid RC, Alonso JM (1995) Specificity of monosynaptic connections from thalamus to visual cortex. Nature 378:281–284.

Reitboeck HJ (1983) Fiber microelectrodes for electrophysiological recordings. J Neurosci Methods 8:249–262.

Sahin M, Bowen WD, Donoghue JP (1992) Location of nicotinic and muscarinic cholinergic and μ-opiate receptors in rat cerebral neocortex: evidence from thalamic and cortical lesions. Brain Res 579:135–147.

Sherman SM, Guillery RW (2002) The role of the thalamus in the flow of information to the cortex. Philos Trans R Soc Lond B Biol Sci 357:1695–1708.

Singer W (1977) Control of thalamic transmission by corticofugal and ascending reticular pathways in the visual system. Physiol Rev 57:386–420.

Staiger JF, Zilles K, Freund TF (1996) Distribution of GABAergic elements postsynaptic to ventroposteromedial thalamic projections in layer IV of rat barrel cortex. Eur J Neurosci 8:2273–2285.

Stoelzel CR, Bereshpolova Y, Gusev AG, Swadlow HA (2008) The impact of an LGNd impulse on the awake visual cortex: synaptic dynamics and the sustained/transient distinction. J Neurosci 28:5018–5028.

Swadlow HA (1995) Influence of VPM afferents on putative inhibitory interneurons in S1 of the awake rabbit: evidence from cross-correlation, microstimulation, and latencies to peripheral sensory stimulation. J Neurophysiol 73:1584–1599.

Swadlow HA, Gusev AG (2001) The impact of "bursting" thalamic impulses at a neocortical synapse. Nat Neurosci 4:402–408.

Swadlow HA, Gusev AG (2002) Receptive-field construction in cortical inhibitory interneurons. Nat Neurosci 5:403–404.

Swadlow HA, Weyand TG (1985) Receptive-field and axonal properties of neurons in the dorsal lateral geniculate nucleus of awake unparalyzed rabbits. J Neurophysiol 54:168–183.

Swadlow HA, Weyand TG (1987) Corticogeniculate neurons, corticotectal neurons, and suspected interneurons in visual cortex of awake rabbits: receptive-field properties, axonal properties, and effects of EEG arousal. J Neurophysiol 57:977–1001.

Swadlow HA, Gusev AG, Bezdudnaya T (2002) Activation of a cortical column by a thalamocortical impulse. J Neurosci 22:7766–7773.

Swadlow HA, Bereshpolova Y, Bezdudnaya T, Cano M, Stoelzel CR (2005) A multi-channel, implantable microdrive system for use with sharp, ultra-fine "Reitboeck" microelectrodes. J Neurophysiol 93:2959–2965.

Vaknin G, DiScenna PG, Teyler TJ (1988) A method for calculating current source density (CSD) analysis without resorting to recording sites outside the sampling volume. J Neurosci Methods 24:131–135.

Weyand TG, Boudreaux M, Guido W (2001) Burst and tonic response modes in thalamic neurons during sleep and wakefulness. J Neurophysiol 85:1107–1118.

Wörgötter F, Suder K, Zhao Y, Kerscher N, Eysel UT, Funke K (1998) State-dependent receptive-field restructuring in the visual cortex. Nature 396:165–168.

Zucker RS, Regehr WG (2002) Short-term synaptic plasticity. Annu Rev Physiol 64:355–405.